

REVIEW

Open Access



# Hyperspectral imaging as an emerging tool to analyze microplastics: A systematic review and recommendations for future development

Andrea Faltynkova<sup>\*</sup> , Geir Johnsen and Martin Wagner

## Abstract

A central challenge in microplastics (MP, diameter < 5 mm) research is the analysis of small plastic particles in an efficient manner. This review focuses on the recent application of infrared hyperspectral imaging (HSI) to analyze MP. We provide a narrative context for understanding technical principles of HSI followed by a systematic review and discussion of the variety of approaches to apply HSI to MP research, including instrumentation, data collection and analysis. HSI was successfully applied to analyze dry MP > 250 µm, with drastic improvements in analysis time as compared with the best available technology, such as Fourier transform infrared (FT-IR) and Raman spectroscopy. Primary challenges we identified through the review include improving spatial resolution to detect smaller MP and development of robust models for data analysis. Parameters and practices for reporting quality assurance and quality control measures are summarized and recommendations are made for future research. We conclude that HSI is a promising technology for MP analysis but requires adaptation for this new application.

**Keywords:** spectral imaging, chemometrics, plastic pollution, method development

## Introduction

Plastics are environmental pollutants ubiquitous in marine and freshwater environments [1, 2] as well as terrestrial ecosystems [2]. While it has been established that plastic pollution can adversely affect non-human organisms [3], the effects on human health are remain uncertain [4]. Distribution of MP is another area of uncertainty. Studies reporting MP presence and abundance are typically local or regional and do not provide enough data to build a global picture [5]. More data on distribution and effects of MP will be required in the coming decades to close these knowledge gaps and mitigate any potential negative effects.

The body of research addressing plastic pollution is rapidly growing, however the analytical detection and

characterization of plastic debris poses a range of challenges: Large debris can easily be captured and analyzed, but microplastics (MP) – often defined as particles with a diameter smaller than 5 mm [6]– pose an analytical challenge [7]. Visual MP analysis is simple and inexpensive, but no longer an acceptable standard, especially for particles smaller than 500 µm. Chemical analytical methods have become an essential part of MP research to provide chemical confirmation of MP as synthetic polymers in addition to identifying MP below 500 µm. High-tech solutions using imaging spectroscopy have become the “gold standard” because of their accuracy and spatial resolution but are time consuming and expensive.

A simple and fast approach is needed to increase sample throughput and make high quality analytical techniques more widely available. Hyperspectral imaging (HSI) has recently been applied to MP analysis with encouraging results. HSI was originally developed for

\* Correspondence: [andrea.faltynkova@ntnu.no](mailto:andrea.faltynkova@ntnu.no)

Department of Biology, Norwegian University of Science and Technology, Høgskoleringen 5, 7491 Trondheim, Norway

remote sensing of the earth's surface [8] but has since been applied to a variety of fields for identification of materials [9–12]. Most notably, HSI is widely used in the recycling industry to separate plastics by polymer type [13]. This is a promising proof of concept with clear links to MP analysis.

This systematic review presents literature which uses HSI for analysis of MP. The goal of this review is to critically assess the capabilities and limitations of this technique and to outline needs for improvement that will facilitate the application of HSI in MP research. The review focuses on technical aspects of data acquisition (spectral resolution, spectral range, spatial resolution, analysis time) and data analysis (chemometric analysis and modelling) to summarize which strategies have achieved the best results. Challenges and advantages of HSI are compared with Fourier transform infrared (FT-IR) and Raman spectroscopy to assess the relative effectiveness of this technique.

#### **Current approaches and challenges in microplastics analysis**

MP analysis of environmental samples can be divided into three distinct processes: sample collection, sample treatment to isolate MP and the identification and characterization of MP to confirm the polymer type of a particle [14]. Sample type will usually dictate the first two processes. The sample matrix represents a general challenge independent of the analytical technique: Separating MP from naturally occurring materials such as tissue, chitin, silica and other minerals requires an elaborate sample preparation, including density separation, enzymatic treatment and wet peroxidation [15]. The last step in the analysis, characterization of MP, will depend on the instrumentation available to the researcher and the research questions of interest. MP characterization has become more sophisticated in recent years as the field of MP research has matured.

Characterization of MP was initially a physical description of the particles. Particles are categorized into size classes which are parsed based on limits that are often more operationally than scientifically motivated [16]. As an example, the mesh sizes of nets and sieves are often the determining factors. The simplest way to identify MP is using visual inspection with the naked eye. Descriptors such as form, color, or resistance to heat (e.g., hot needle test) can be used to tentatively confirm particles as plastics [17]. This process provides some quantitative and qualitative description of the particles; however, it is based on the subjective evaluation of the analyst [18]. Even experienced analysts can misclassify particles resulting in an overestimation [19] or underestimation [20] of the number of MP in a sample. Lastly and perhaps most importantly, it is impossible to

confirm the chemical composition of the particle. For these reasons, visual identification can be useful as a simple tool available to many but cannot be used to quantify MP with high accuracy or repeatability.

Analytical techniques which can identify the polymer type are now generally preferred [14, 21]. One technique to characterize polymers in environmental samples is pyrolysis-gas chromatography coupled to mass spectrometry (Py-GC-MS) [22]. Py-GC-MS uses controlled thermal degradation to convert solid samples into pyrolysis products that are separated by gas chromatography and identified using mass spectrometry. Most polymers will yield unique pyrolysis products [23] enabling the simultaneous identification of multiple synthetic polymers in a sample. Py-GC-MS can thereby provide information regarding the presence of different polymers and an estimate of their mass-based concentration according to their degradation products. A major benefit of Py-GC-MS is sensitivity; nanoplastics can be quantified even in low quantities [24]. It should however be noted that the accuracy of concentration estimates has been questioned [24]. A limitation of Py-GC-MS is that qualitative and quantitative information about the particles is lost (e.g., number, size, and shape of MP) due to the thermal degradation of the sample. To avoid losing morphological information, Py-GCMS can be combined with other analytical techniques. Spectroscopic techniques can be used to analyze a sample before it is analyzed with Py-GC-MS (i.e., before the sample is destroyed). This provides detailed information about the particle characteristics of MP [25], in addition to detailed chemical information and mass estimates from Py-GC-MS.

Like Py-GC-MS, Raman and FT-IR spectroscopy can chemically identify MP [26]. Both are optical, non-destructive techniques and are routinely used for MP analysis. Raman spectroscopy has reportedly detected particles as small as 1  $\mu\text{m}$  [27], while FT-IR techniques have a limit of detection of 10–20  $\mu\text{m}$  [28]. In their simplest forms, both techniques use point measurements to analyze particles. If particles are large and easy to handle, these methods work well and can identify polymer type relatively quickly [21]. However, manual selection of particles can still result in some selection bias; suspected MP can be ruled out as false positives, but it is impossible to know how many particles were incorrectly classified as non-plastic (i.e., missed or overlooked).

For particles < 500  $\mu\text{m}$ , manual handling becomes impractical and particles must be analyzed on a filter where a sample has been deposited. In this case, the operator must locate particles on the filter (usually with a microscope attachment) and take a point measurement of each particle to confirm its chemical composition. To reduce bias of particle selection and additional manual

work, software-based solutions such as ParticleScout and ParticleFinder can automatically select particles based on bright or dark-field imaging [29]. A microscope is used to image a portion of the filter's area and an image recognition algorithm automatically highlights all particles in the field of view (FOV). Each particle identified by the software is systematically analyzed with the help of a motorized stage. The stage moves to the desired region and a point measurement is taken with the laser (Raman) or IR beam (FT-IR). All points identified by the algorithm as "particles" will thus be sampled. An automated approach using particle identification software is less subjective and reduces the chance of missing MP. However, in samples with many particles this approach can be time consuming. The analysis time is dependent on the number of particles identified in the image. Depending on the sample medium and treatment, organic, mineral or biological matter could be present during analysis. This increases the number of particles to be analyzed, adding to analysis time.

Another approach to automated analysis is the use of spectral imaging techniques based on FT-IR and Raman spectroscopy. Focal plane array FT-IR (FPA-FT-IR) and Raman imaging stitch together photomosaics from multiple small areal measurements. The result is a spectral image where each pixel contains a Raman or FT-IR spectrum. This technique removes particle selection altogether, relying on full coverage of the filter surface area to capture all particles. Areas of the filter that contain specific polymer spectra are identified using matching algorithms or chemometric analysis [30].

Imaging techniques remove selection bias but introduce a new obstacle: areal coverage. For example, the focal plane arrays of FT-IR instruments cover very small areas (approximately  $5.5 \mu\text{m}^2$  depending on the sensor), while filters are often 47 mm in diameter. With a filter of this size, the sample covers an area of circa 1700  $\text{mm}^2$ . As a result, analyzing an entire sample is highly time consuming. With the best available instrumentation, analysis time for one  $14 \times 14 \text{ mm}$  area is currently four hours [28]. Therefore, FPA-FT-IR is often applied to a small subset of the filter area and the results are extrapolated to the total filter area [21, 31, 32]. Such an approach assumes that any given area of a filter is representative of the whole sample and MP are homogeneously distributed on the filter. Because this is not generally the case, imaging subsets of samples introduces additional uncertainty [33].

In addition to being time consuming, both Raman and FT-IR imaging systems are highly complex and expensive with costs in the range of 100 k to over 200 k USD, respectively [28]. In addition, imaging systems such as FPA-FT-IR operate in transmittance mode. This requires specialized sample filters that are IR transparent and

very flat (such as aluminum oxide membrane filters) [33] which adds to expenses for consumables. Operation in transmittance mode also excludes particles which are entirely opaque or very thick, as the signal will be attenuated completely [28, 30, 32]. Opaque particles can be identified with Raman imaging, but fluorescence from organic matter can hinder identification [30].

HSI has recently been applied to analyze MP and shares many characteristics with FPA-FT-IR (see 1.5). With HSI, an entire filter can be imaged precluding the need for particle selection or analysis of smaller areas of the filter. As with FPA-FT-IR and Raman imaging, the output of HSI is an image which contains a spectrum for each pixel. The spectra are classified with multivariate techniques to identify chemical signatures of objects in the image. The image can thus provide quantitative and qualitative data about the polymer type of MPs, their size, number, and shape (Fig. 1).

#### What is a hyperspectral image?

The term "hyperspectral imagery" was coined by Alexander F. H. Goetz in a 1985 paper on remote sensing which describes the inception of the technology [8]. HSI was developed as an imaging technique to identify materials on the earth's surface from air and space craft. HSI provides high spectral resolution as compared with multispectral imaging systems such as the Landsat multispectral scanners. This improvement in spectral resolution enabled improved identification of surface materials, specifically minerals in soils. The copious amounts of data also helped to overcome challenges in remote sensing such as atmospheric interference and multiple mixed materials on the earth's surface [34]. Despite being developed in the 1970s, HSI did not see wide application until technical advances allowed easier data storage and processing [34].

Since the 1980s, HSI has been applied in a broad spectrum of fields. Remote sensing with HSI has been applied underwater and in space [9, 35, 36]. The medical field uses HSI to identify tissues such as nerves, cancer cells and burn wounds [11]. Food processing industries use HSI for quality control of produce [10]. Waste processing plants use HSI to sort wastes, specifically in the recycling of plastic materials [13]. Sorting plastic waste into categories by polymer type results in higher quality polymers for recycling. In this specific case, the same principles applied in recycling can be applied to MP in environmental samples. On a larger scale, remote sensing has been used to identify macroplastics in the environment from airplanes, drones, and satellite images [37–41].

A hyperspectral image is based on the same principles as a traditional red-green-blue (RGB) image. An image can be represented as a matrix with I rows and J columns, giving the dimensions I x J. These two spatial

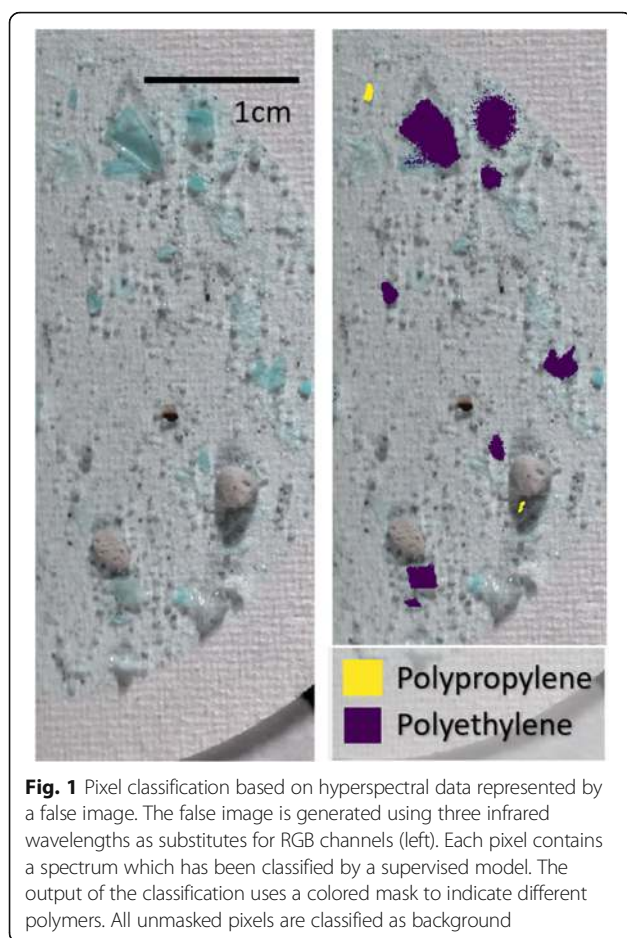


**Fig. 1** Pixel classification based on hyperspectral data represented by a false image. The false image is generated using three infrared wavelengths as substitutes for RGB channels (left). Each pixel contains a spectrum which has been classified by a supervised model. The output of the classification uses a colored mask to indicate different polymers. All unmasked pixels are classified as background

dimensions are the size of the image. Each entry in the matrix is synonymous with one pixel. Despite the use of squares to represent pixels, pixels are in fact point measurements [42]. These “squares” are more correctly referred to as the spatial resolution, where each point measurement (pixel) represents an area of a discrete size. Each pixel represents a position in real space which is reflecting and absorbing light across the electromagnetic spectrum. Reflected light is registered as a number indicating the intensity. If only one wavelength is sampled, the result is a greyscale image where high intensity is represented as white and low intensity as black. A color image uses three wavelength bands to describe the amount of light in a *region* of the electromagnetic spectrum which is being reflected by an object. These color bands lie within the spectrum of light visible to the human eye (400–800 nm) and correspond to red, green, and blue visible light. These regions are chosen due to the human eye’s sensitivity to these photopigments. Each pixel in an image is expressed as a combination of three intensity values representing red green and blue (RGB), and the matrix now has three dimensions [43]. *I* and *J* are spatial as before, and the new third dimension, *K*, is

spectral. The three *K* components can be visualized as layers with dimensions *I* × *J* stacked against one another.

If more layers are included, the visible spectrum can be more finely parsed to include multiple narrower bands thereby providing more detailed information. This is called a multispectral image. Both the number of bands and the width of the bands can vary. Since the human eye only needs three wavebands to interpret color, the addition of multiple spectral bands is not done for viewing pleasure. It is rather a more detailed representation of how an object reflects light and can give information about the chemical composition of that object. Sampled wavelengths can include regions of the electromagnetic spectrum other than visible light, such as the infrared (IR), to target absorbance regions of specific chemical bonds. The resulting data takes the form of a three-dimensional datacube with field of view of the imager (*I* × *J*, i.e., pixels) and the number of wavebands (*K*).

When the number of spectral bands is larger than 100, the resulting datacube becomes hyperspectral. The seminal paper describing HSI by Goetz et al. [8] defines HSI as “the acquisition of images in hundreds of contiguous, registered, spectral bands such that for each pixel a radiance spectrum can be derived”. This definition excludes multispectral imaging as the bands are not necessarily contiguous. The result of this contiguous sampling is best viewed as a spectrum. This spectrum is a highly detailed representation of the different wavelengths of light reflected by an object, and therefore allows classification of pixels according to chemical composition rather than just color.

### Hyperspectral instrumentation

The main components of a hyperspectral imager consist of an objective lens (i.e., a fore lens, front optic or camera lens), a spectrograph with an entrance slit (of fixed width) and a two-dimensional detector which is typically a photovoltaic semiconductor, such as a charge-coupled device (CCD). A light source is also a key component but is not typically integrated with the imager. An ideal light source is a National Institute of Standards and Technology (NIST) issued tungsten halogen lamp which emits strongly in both visible and IR light. The characteristics of the components will influence the measurement parameters such as spatial and spectral resolution, bandwidth, bit depth and signal-to-noise ratio.

There are three common methods of HSI image acquisition: the point scan, line scan or areal scan. Of the three methods, (see [44] for in-depth discussion), the line scan or “pushbroom” method/sensor has become the method of choice for many applications of HSI, such as remote sensing [38, 45, 46]. The pushbroom scan uses the movement of either the object being imaged or the



imager to cover a given area (Fig. 2). The pushbroom is a line-scan technique that collects one “line” in the spatial dimension per measurement, (i.e., slit image). The light source is above the sample pointing downwards. As the light source does not emit the same intensity of light at each wavelength, a Lambertian reflectance standard (e.g. Labsphere Spectralon) is used to correct the spectra. The reflectance standard reflects all wavelengths equally, and thus records the emission spectra of the light source. Light from the source hits the object being imaged and is reflected upwards where it passes through the foreoptic and slit. The beam then passes through to a collimator followed by a dispersive element [47]. The dispersive element spatially separates each wavelength which is then focused onto a 2D detector array. In this case, one spatial dimension and the spectral dimension ( $I'K$ ) are sampled simultaneously. By moving the imager, an adjacent area can be sampled giving the second spatial dimension ( $J$ ). The line scan is perpendicular to the direction of movement. The frame rate corresponds to the speed of movement and each line is stitched to the next creating a photomosaic of slit images. The slit size is fixed, but by moving the imager closer to or farther away from an object, the height of the line scan can be changed. The same is true for the width of the line which is always limited to one pixel. That is to say that the area imaged by one detector diode (and thus spatial resolution) is dependent upon the distance between the imager and the object of interest as well as the FOV.

#### Key differences to FT-IR spectroscopy

Raman spectroscopy operates on different principles than IR spectroscopy, but both FT-IR and HSI can be used to obtain reflectance or transmittance spectra in IR. The key differences lie in the instrumentation used to collect these spectra, and their limitations with respect to time, areal coverage, and spectral range. Most FT-IR instruments use an interferometer to obtain spectra in which a moving mirror creates constructive and destructive interferences of wavelengths over time [48]. To sample all wavelengths in a given range, the mirror must be displaced a given distance. This single “scan” (i.e., movement of the mirror through its decided range) is repeated and the final spectral output is often an accumulation of multiple scans [48]. Each measurement produces a spectrum from a single point. Rather than using interference patterns to separate wavelengths, HSI instruments use dispersive elements and sensor arrays as described above. This allows HSI to cover larger areas in less time compared to FT-IR instruments.

The spectral range of HSI and FT-IR also differ. FT-IR spectra often cover the range of  $400\text{--}4000\text{ cm}^{-1}$  equivalent to wavelengths of  $2500\text{--}25,000\text{ nm}$ . This wide spectral range gives information about a variety of polarizable

chemical bonds including characteristic peaks for functional groups and influences of hydrogen bonding. HSI focuses on a smaller range of wavelengths, typically visible light ( $400\text{--}700\text{ nm}$ ) and the near infrared region from  $700\text{ nm}$  up to  $2500\text{ nm}$ . This limits the information in one spectrum, but the infrared region of  $1700\text{--}1800\text{ nm}$  captures the characteristic first overtone of the C-H bond useful for identifying organic molecules [49].

FT-IR and HSI ultimately produce the same type of information (spectra in IR), but the differences in instrumentation separate the two technologies with respect to analysis time and detail of information. FT-IR gives a more detailed spectrum at the cost of a more time-consuming procedure. HSI spectra have a narrower spectral range but imaging large areas can be done in minutes. Exactly how much nuance can be sacrificed for speed is a central question is assessing how HSI can be used for MP analysis. This and other issues concerning availability of instrumentation, data processing and performance are the central focus of the systematic review.

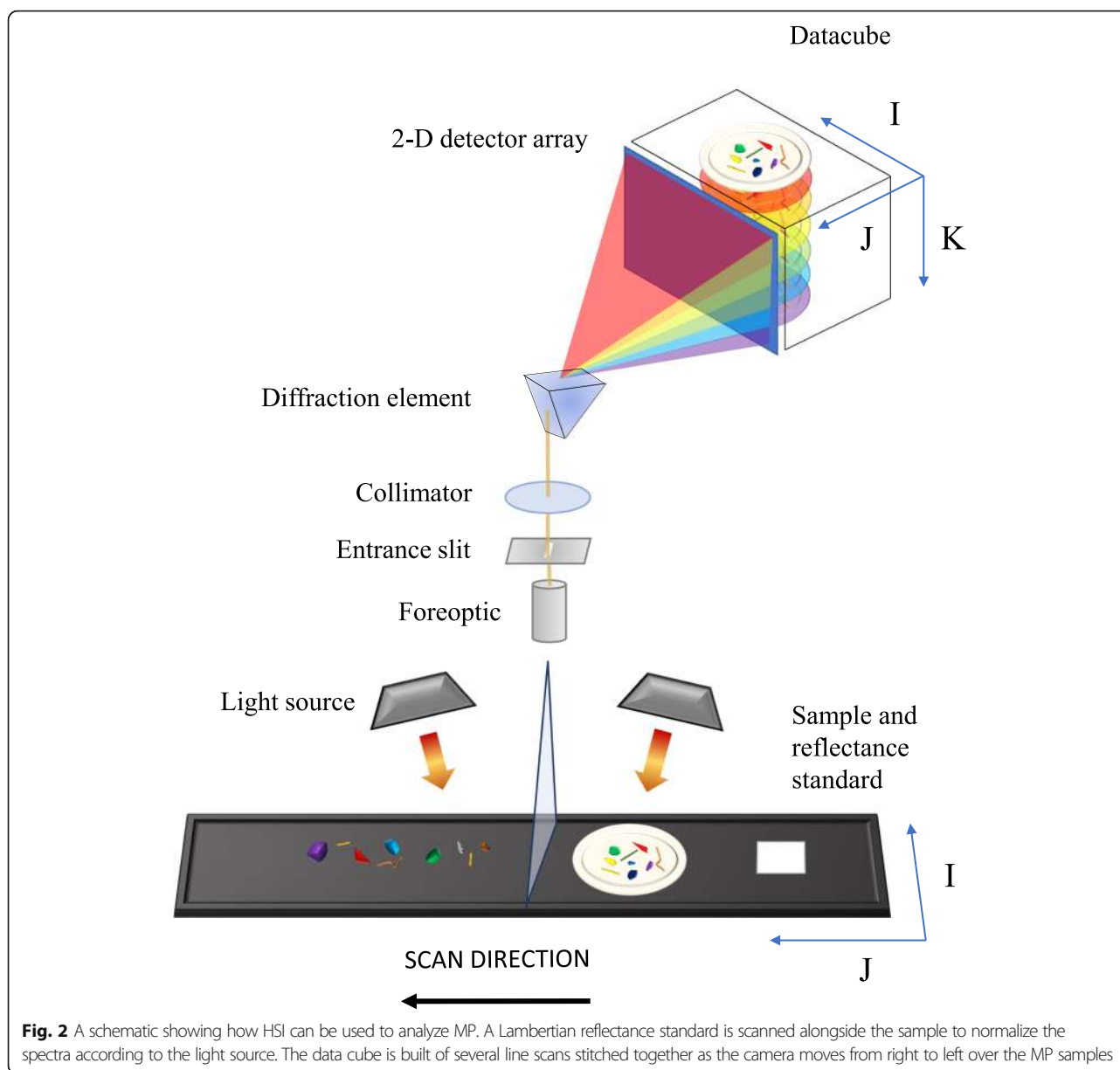
## Methods

### Literature search

The methods and criteria used for the literature search and selection process are described in a dedicated protocol published on Zenodo [50]. The protocol follows the Preferred Reporting Items for Systematic Reviews and Meta-Analyses (PRISMA) [51] recommendations for systematic reviews. PRISMA guidelines have been adapted to reflect the current field of research. The literature search was carried out in May 2020. Three databases (Scopus, Web of Science and ScienceDirect) and four keyword combinations were chosen to search for relevant literature. The keywords included 1) microplastic\*, 2) macroplastic\* OR “plastic litter” OR “plastic debris”, 3) hyperspectral, 4) “imaging spectroscopy” OR “spectral imaging”. These four terms were combined as follows:  $1 + 3$ ,  $1 + 4$ ,  $2 + 3$ ,  $2 + 4$  (Table 1).

All publications returned by the search were pooled in an Endnote database. Preliminary title and abstract screening was used to exclude obviously irrelevant literature. The literature was then further screened and categorized into three levels (hereafter referred to as level 1, level 2 and level 3) by two authors independently using the online platform Rayyan QCRI [52]. Classification disagreements among the authors were discussed and agreement was reached after reading the full texts.

Level 1 studies are included in the systematic review and apply HSI either to identify micro- or macroplastics in environmental samples or in laboratory experiments using simulated MP to optimize this application using spiked samples. Literature using other spectroscopic techniques without an imaging component (i.e. point measurements) such as spectroradiometers and



spectrometers were excluded. Level 2 publications are tangentially relevant to the subject area and include reviews of analytical methods if they include HSI and remote sensing applications of HSI for plastic pollution. The full texts are reviewed for relevant details and resulting contributions are discussed. Level 3 publications are excluded from the review. This includes waste management applications of HSI, studies using FT-IR or Raman spectroscopy only, books and book sections as well as material not in English.

#### Study evaluation

The purpose of this review is to collect information on the suitability of HSI for MP analysis. More broadly speaking,

the field of MP research is currently making efforts to harmonize and standardize protocols for quality assurance and quality control (QA/QC). There are no standard reference materials available, and research groups typically develop QA/QC guidelines internally. While some descriptions of best practices are available [53], they are not seen as highly relevant for exploring the feasibility of HSI as a MP analysis method. The diversity of methods, approaches and challenges is the primary theme of this paper; therefore, we chose not to evaluate the quality of the studies based on any QA/QC criteria.

For level 1 publications, metadata such as journal, author and year of publication was collected, along with the following information: Type of study (identification of MP

**Table 1** Search terms and number of results based on search engine

Search term	Scopus	Web of Science	ScienceDirect
Microplastic* AND hyperspectral	140	17	56
Microplastic* AND ("imaging spectroscopy" OR "spectral imaging")	50	6	22
(macroplastic* OR "plastic litter" OR "plastic debris") AND hyperspectral	98	12	41
(macroplastic* OR "plastic litter" OR "plastic debris") AND ("imaging spectroscopy" OR "spectral imaging")	35	3	16

in environmental samples or method optimization using known MP), sample matrix (if applicable), number and type of synthetic polymers identified, size of MP analyzed, instrumentation type and technical specifications (spectral range and resolution, spatial resolution, limit of detection), analysis time, data processing strategy and cost of instrumentation.

## Results & Discussion

### Systematic Literature review: overview of studies

The literature search returned 496 results of which 224 were unique publications after the removal of duplicates (Fig. 3). The abstract and title screening resulted in 114 potentially relevant publications. Twelve studies were categorized as level 1 and thus included in the systematic review (Table 2). Seventy studies were categorized as level 2, including 43 reviews and 27 studies on remote sensing of plastics. Thirty-three publications were excluded (level 3) because they did not apply HSI techniques, did not analyze MP or dealt only with the theoretical aspects of data processing.

HSI used for MP analysis is an emerging field in the early phases of development. This is reflected in the fact that all level 1 studies were published between 2016 and 2020. These studies can be divided into those which collect and analyze samples from the environment ( $n = 8$ ) and those which focus on method development using MP made in the laboratory ( $n = 4$ , Table 2). One method study is a combination of both, analyzing micro- and macroplastics from the environment and spiked samples in artificial media.

In the reviewed studies, four environmental media were sampled: seawater ( $n = 5$ ), soil ( $n = 1$ ), sand ( $n = 1$ ) and biota ( $n = 1$ ). Focus on the marine environment is consistent with what we see in the literature with respect to other MP studies [4]. Much like Raman and FT-IR spectroscopy, HSI focuses on the analysis of particles after sample treatment to remove the interfering matrix. The number of polymers identified ranges from 1 (in studies where other characteristics such as color or size are the focus) to 13. Polymer types often included polyethylene (PE), polypropylene (PP) and polystyrene (PS). Authors also report the number of MP particles as well as polymer type [54–61, 64], particle size [58, 61, 64] and particle morphology [58, 61]. This demonstrates the ability of HSI analysis to provide both qualitative and

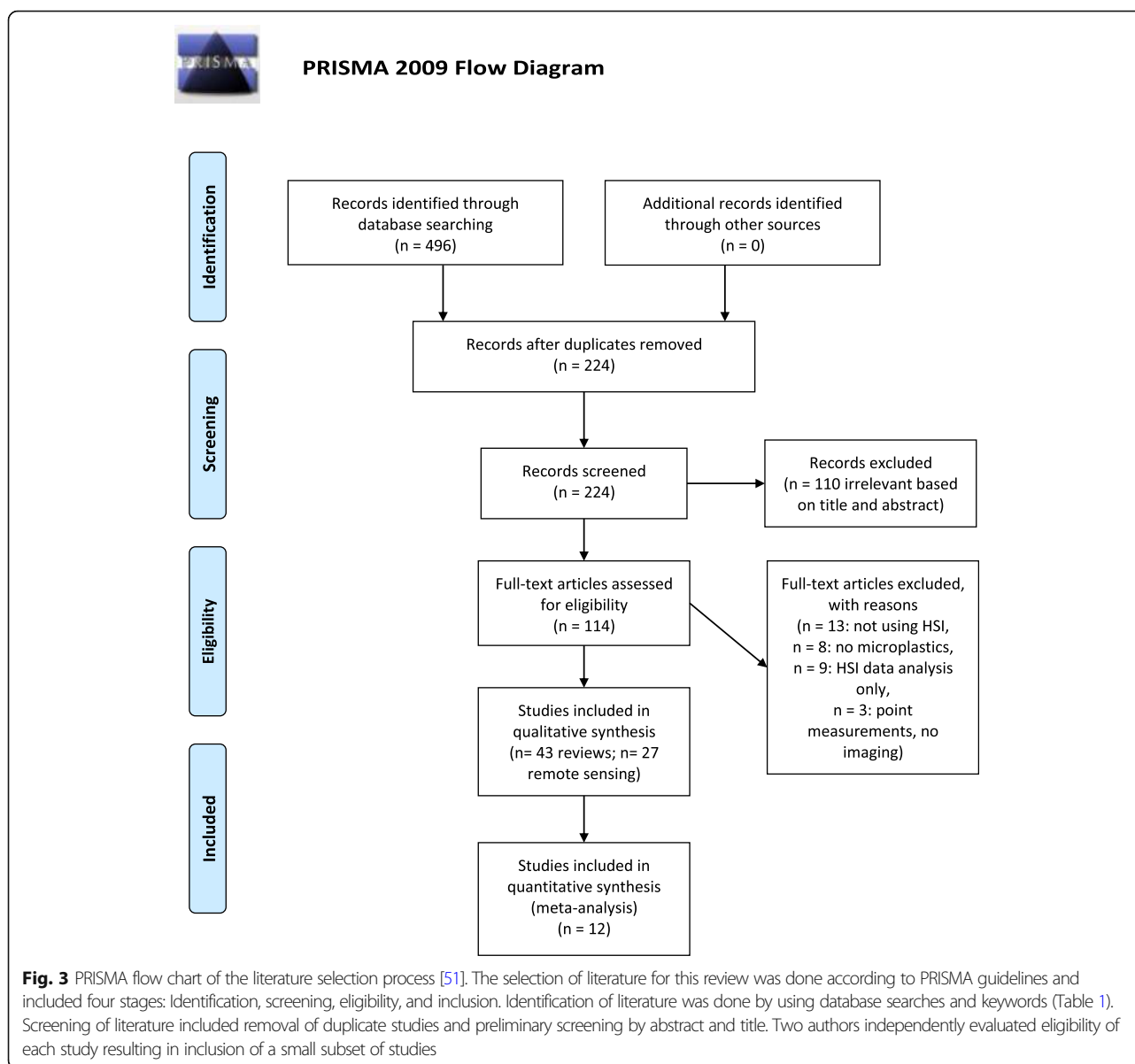
quantitative data for MP particles. Not all studies included both qualitative and quantitative data, presumably because extracting particle number and morphology requires more comprehensive image analysis than just identification of presence/absence of certain polymer types (see 3.7).

### Sample collection and preparation

Seawater was collected with either manta trawls of surface water using 300–500  $\mu\text{m}$  mesh nets [54, 55, 57, 58], multiple Niskin bottles [56], or a sea water pump connected to a filtration unit. Soil and sand samples were collected from quadrats [59, 60], while the intestinal tracts of crucian carps were collected from fresh market fish [61]. Sample preparation varied with each study based on the sample matrix. There was noted variation even when the sample matrix was the same: Some seawater samples were treated with combinations of enzymes, hydrogen peroxide and filtration or not treated at all. Density separations were used in the case of soil and sand samples to isolate MP. In method development studies [62–65] pristine plastic pellets (i.e. virgin plastic) were purchased from a manufacturer or acquired from a research institution. To simulate MP which were not only pristine pellets, common plastic items such as water bottles were cut into smaller pieces.

Regardless of sample treatment, all MP were ultimately either manually transferred into a separate container (often a petri dish) or filtered onto a glass fiber filter with a small pore size (ca. 2  $\mu\text{m}$ ). The former method is used primarily for particles larger than 500  $\mu\text{m}$  that have been visually identified as potential MP. Large particles which are practical to handle were often positioned on a black background for imaging. This provides greater contrast and can be used as an additional class in supervised analysis (see 3.7). Particles smaller than 500  $\mu\text{m}$  were filtered onto glass fiber filters or filters of another suitable material. The filter with the deposited sample was then imaged by HSI. Both approaches (selection/arranging of particles and deposition on a filter) are illustrated in Fig. 2.

The analytical method will dictate which filter materials are suitable. Ideally, HSI methods can be validated against either Raman or FT-IR spectroscopy. The filter material should therefore be compatible with multiple methods. Zhu et al. [65] discuss the use of different filters to



improve detection and classification of MP and found that gold-coated polycarbonate filters improved spectral characteristics of PE particles compared to glass fiber filters. If using glass fiber filters, filters without binders are recommended as binders can produce their own spectral signatures which interfere with measurements. For comparisons to Raman spectroscopy, both gold-plated and glass fiber filters are suitable. For transmission measurements with FT-IR systems, aluminum oxide membrane filters are recommended by Löder et al. [33]. HSI spectra of Anodisc or other aluminum oxide filters have yet to be analyzed. Confirming their suitability would allow direct comparisons between FPA-FT-IR and HSI.

Based on the studies covered in this review, we can conclude that a glass fiber filter without binders provides

a suitable background for HSI measurements and is the least expensive option. Unless the goal of the research is to compare HSI with FT-IR in transmission mode, glass fiber filters are recommended for particles well above the spatial resolution of the instrument. As particle size approaches the spatial resolution of the hyperspectral camera, gold-plated filters may provide better results.

#### Instrumentation

Eleven different hyperspectral cameras based on the pushbroom method were used to produce hyperspectral datacubes in the reviewed studies (Table 3). While 11 of the 12 studies only use one HSI camera, Karlsson et al. [55] used three different hyperspectral imagers and compared their performance. The wide variety of



**Table 2** Articles included in the systematic review. Some authors analyze plastic particles in environmental samples while others use spiked samples for the development of HSI methods. Size ranges given in  $\mu\text{m}$  were not always completely reported and thus some are reported as either a maximum or minimum size analyzed by the authors

Type of study/sample	MP size range collected/analyzed ( $\mu\text{m}$ )	Collection method/origin of particle	Sample clean-up/preparation	Reference
Seawater	300–500	Manta trawl	Size fractionation, enzymatic digestion, peroxide oxidation, filtration	[54]
	250–5000	Manta trawl	Visual selection	[55]
	> 63	Niskin bottle	Ethanol, peroxide oxidation, filtration	[56]
	> 333 (trawl) > 50 (pump)	Manta trawl and in-situ pump	Visual selection	[57]
	> 500	Manta trawl	No description given	[58]
Sand/soil	> 100	Quadrat sample	Size fractionated, collected in petri dish	[59]
	500–5000	Quadrat sample	Density separation, visual selection	[60]
Biota	100–1000	Purchase of fish from local market	Rinsing & scraping of intestinal tract, smear on Teflon plate	[61]
Methodology study	180–647,000	Pristine pellets purchased from manufacturer, collection of urban waste	Manually cut or milled into smaller particles	[62]
	< 2	Polymer matrix synthesized in lab	Photodegradation to produce nanoparticles	[63]
	200–3000	Pristine pellets purchased from manufacturer; local household items collected	Grinding and size fractionation by metal sieve or manual cutting	[64]
		Manta trawl in seawater	Filtration of seawater samples	
	100–5000	Pristine pellets and large plates purchased from manufacturer	Manually cut into smaller particles	[65]

instruments shows that HSI for MP analysis is a developing application. Different research groups are experimenting with different systems which are usually designed for other applications such as waste sorting. While this is not a harmonized approach, it has the benefit of allowing comparisons between instruments and methods applied.

### Spatial resolution

Spatial resolution, that is, the smallest area represented by one image pixel, is a critical parameter considering the trend towards analysis of smaller MP. However, there is no uniform reporting of the spatial resolution in the available literature: Some studies either did not report it at all or use a variety of similar but not analogous terms. It is important to report spatial resolution in technically correct and relevant terms to accurately communicate the capabilities of HSI. As an example, some authors report “pixel pitch” as analogous to spatial resolution. Pixel pitch denotes the distance between pixels on a camera sensor or screen and thus has a proportional relationship to the area being imaged. However, pixel pitch alone does not contain enough information to derive the size of the area represented by one pixel. To calculate this area, one also needs to report the distance to the object, the FOV of the foreoptic and the number of pixels on the sensor.

To facilitate the comparison of HSI instrumentation and studies, reporting the spatial resolution as the area represented by one pixel in an image is preferable and recommended. This value should be reported as a set of dimensions (height and width), as pixels are not necessarily square. In addition, the limit of spatial detection is a useful parameter to report because it represents the size of the smallest particle that can be detected. An important distinction is that spatial resolution is not always synonymous with limit of detection (LOD). As reported by Schmidt et al. [56], two adjacent pixels needed to be classified as the same synthetic polymer to reduce false positives (see section 3.7). As a result, any particles smaller than two pixels will not be detected. Spatial resolution and data processing are thus both contributing factors to LOD.

In the studies reporting spatial resolution, the values vary from 0.13–1000  $\mu\text{m}$  (smallest possible dimension represented by one pixel). Gallagher et al. [63] used a CytoViva dark-field HSI microscope which has the highest spatial resolution of all instruments used. The authors did not outline the exact specifications but based on their RGB images the image pixel size represents an area of less than 2  $\mu\text{m}^2$ . According to the manufacturer, CytoViva hyperspectral microscopes can achieve spatial resolution down to 0.128  $\mu\text{m}$  [66], which would imply an improved LOD as compared with the current performance of Raman spectroscopy (LOD = 1  $\mu\text{m}$ , [27]). More

**Table 3** Technical specifications of benchtop HSI instrumentation used to analyze MP

Instrument (manufacturer)	Wavelength range (nm)	Spatial resolution ( $\mu\text{m}$ )	Spectral resolution (nm)	# polymers identified	Reference
Hypex SWIR 320 hyperspectral camera (Norsk Elektro Optikk)	968–2498	280	6 <sup>a</sup>	11	[54]
				13	[56]
SISU Chema XL (SISU Chema)	1000–2500	100	6.3	4	[59]
			5.9 <sup>a</sup>	3	[58]
Umbio Inspector (SISU Chema)	1000–2500	300	5	12	[55, 57]
V-NIR-A (Headwall Photonics)	400–1000	NR	2 <sup>b</sup>	1	[60]
V-NIR (Headwall Photonics)	900–1700	NR	3 <sup>b</sup>	5	[61]
G4-428 Hyperspec NIR R (Headwall Photonics)	900–1700	NR	3 <sup>b</sup>	3	[64]
Pika NIR-640 (Resonon Inc.)	900–1700	14.8	2.5	11	[65]
Malvern InGaAs camera (Malvern Panalytical)	960–1662	300, 1000	5.9 <sup>a</sup>	12	[55]
Videometer instrument (Videometer AS)	375–970	60	31.3 <sup>a</sup>	12	[55]
Dark field CytoViva hyperspectral microscope (Cytoviva)	400–1000	0.128 <sup>b</sup>	2	1	[63]
NIR Specim Inspector spectrometer mounted in front of an InGaAs Sensor Unlimited camera	350–2000	25	10	9	[62]

<sup>a</sup>Calculated from spectral range and sampled wavelengths, <sup>b</sup> Details from manufacturer, NR not reported

recent publications use dark-field hyperspectral microscopy ( $\mu\text{HSI}$ ) to identify MP in organisms. Nigamatzyanova and Fakhrullin [67] identified MP with a diameter of 100 nm in vivo in *C. elegans*. Nigamatzyanova and Fakhrullin [66] note that separation of particles from the matrix is not possible, as the aim is to visualize MP in tissues or cells. The tissues of interest must be localized in the FOV, and MP analyzed without prior extraction or up-concentration. Identification of MP particles in tissue was also demonstrated by Mattsson et al. [68] who detected nanoplastics in the brain tissue of fish.  $\mu\text{HSI}$  can clearly be successfully applied for nanoplastics detection, however it cannot be used to analyze a wide range of MP sizes [69].

Aside from  $\mu\text{HSI}$ , instruments used in other studies are generally designed for analyzing larger objects. Still, the next best spatial resolution is 14.8  $\mu\text{m}$  [65]. The authors combined a Pika-640 hyperspectral imager with an extension tube to improve the initial spatial resolution by a factor of 17. This is competitive with methods like  $\mu\text{FT-IR}$  (LOD = 10–20  $\mu\text{m}$ , [28]), but not Raman spectroscopy. Accordingly, modification of instruments with stereomicroscopes or phototubes may be a promising and simple way to further improve their spatial resolution. Examples from other fields also suggest that modifications to existing hardware could improve spatial resolution. Volent et al. [70] mounted a hyperspectral imager to a stereomicroscope for taxonomic identification of macroalgae. Only the visible region of the electromagnetic spectrum was used in this case. When applying this approach to the IR region, IR transparent materials would be required for optical components.

Overall, HSI instruments that are not coupled to microscopy have an average spatial resolution of 285  $\mu\text{m}$  which is comparable to ATR-FT-IR (Fig. 4). Compared to ATR, the benefit of HSI is that all particles can be analyzed simultaneously. This drastically reduces analysis time and precludes the need to physically transfer particles. This in turn reduces the risk of damaging or losing the particles. In addition, some particles are not well suited to ATR since analysis requires good contact between the sample and a crystal for the measurement to be carried out. Regardless of shape or surface structure, MP > 285  $\mu\text{m}$  are well identified by HSI. However, it is important to remember that current HSI technologies are designed to analyze objects much larger (waste sorting) or much smaller (nm scale) than MP. Thus, a hyperspectral imager with a “Goldilocks” spatial

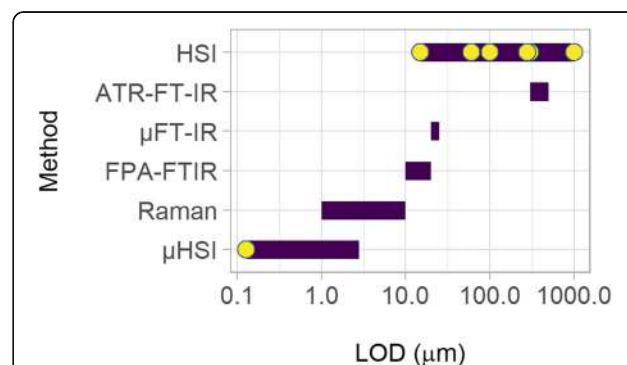


**Fig. 4** Limits of detection of optical analytical methods for MP. Purple bars indicate ranges reported for various analytical methods in other reviews focusing on MP analysis. Yellow dots indicate LODs as reported by the authors of studies included in this review

resolution for MP that covers a range of 10–500  $\mu\text{m}$  remains to be designed.

### Spectral range and resolution

Spectral range and resolution are important parameters to optimize as they yield the quantitative and qualitative information needed to identify plastics. Accordingly, the spectral range must include regions of the electromagnetic spectrum where polymers show distinct absorbance and reflectance patterns.

All but two studies used wavelengths of approximately 900 nm or longer, up to 2500 nm. (Table 3). The two remaining studies focus on shorter wavelengths around 375–1000 nm [60, 63]. Based on the reviewed studies, we identified specific regions of the IR spectrum that contain distinct features useful for separating synthetic polymers (Fig. 5). These regions are found predominantly between 1000 and 1700 nm. This agrees with Karlsson et al. [55] who concluded that the region between 375 and 970 nm was insufficient for polymer classification and, thus, recommend using wavelengths above 1000 nm.

Resolution in the spectral domain varied considerably (1–31 nm) and had an average of 6 nm (Table 3). The coarsest resolution (31 nm) covered 19 wavelengths which was deemed insufficient for polymer classification [55]. Zhu et al. [65] use a resolution of 2.5 nm which revealed more detailed spectral features as compared to 3 and 6 nm used by Shan et al. [64] and Serranti et al. [58], respectively. Clearly, higher spectral resolution has the advantage of providing more detailed information, which facilitates polymer identification. However, this also generates larger datafiles and requires more expensive instrumentation. Thus, the spectral range and resolution must be optimized to reduce computational and instrumental costs. As seen above, the spectral region of 1000–1700 nm contains robust information for classification of polymers and a spectral resolution of 6 nm

may be sufficient [58, 64]. It would be advantageous to compare classification results including and excluding the 1700–2500 nm range to assess the importance of these wavelengths in polymer classification. If this region does not add any critical information, it would be beneficial to simplify data collection and analysis by excluding it. However, spectral range and resolution need to be adapted to the aims of the research.

If the objective is to differentiate between plastics and other materials, a lower spectral resolution may be acceptable. In the context of remote sensing, instruments which are mounted to air and spacecraft have limited data storage and transfer capabilities. This challenge could be overcome by sampling fewer wavelengths to reduce data dimensionality. As an example, Hibbitts et al. [71] use dual wavelength imaging (i.e., only two wavelengths) at 1530 and 1720 nm to identify plastics in a remote sensing context. They concluded that this was insufficient to identify individual polymer types but acceptable for classifying plastics vs. non-plastics. Accordingly, a higher spectral resolution will be needed if the objective of a study is to differentiate polymer types with relatively similar spectral signatures. An interesting concept to explore would be the sampling of key bandwidths as opposed to sampling an entire range of wavelengths, leading to a more multi-spectral as opposed to hyperspectral approach. This could further simplify computational and instrumental requirements.

### Analysis time and cost

The price of an HSI instrument depends on the type of system. As an example, an IR-hyperspectral camera can cost approximately 50 k USD (Resonon Pika-NIR-320), while a benchtop system with an integrated moving stage and software brings the price up to 70 k USD. Information about the cost of HSI microscopy was unavailable, but such systems are certainly more costly. Raman and FT-IR imaging, the gold standard in MP

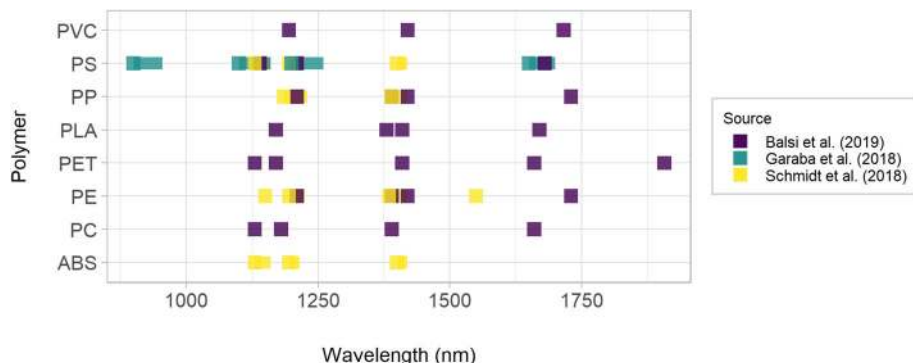


**Fig. 5** Spectral regions useful for identification of various polymers. Ranges indicated by colored bars were identified as containing useful spectral features for the identification and differentiation of polymer spectra. This can include local minima and maxima. PVC: polyvinyl chloride, PS: polystyrene, PP: polypropylene, PLA: polylactic acid, PET: polyethylene terephthalate, PE: polyethylene, PC: polycarbonate, ABS: acrylonitrile butadiene

research, cost approximately 200–250 k USD, more than twice as expensive as an HSI benchtop system [28].

Initial purchasing costs are an important aspect to consider, but cost in terms of analysis time is equally as important. Analysis time is dependent on the area of the image. We will refer to area of the image as height  $\times$  width, meaning that height and width are both spatial dimensions. Hyperspectral imagers which use the pushbroom method have a fixed slit size. The slit size in combination with the distance between imager and object will determine the image height. This is maintained constant as the image is being captured. The width of the image is determined by the distance the imager or object moves during a scan. That is to say that longer scans will result in wider images (larger photomosaics). The length (in time) of the scan (and thus width of the image) is often adjustable by the operator.

For the studies covered here, the scan time ranged from 0.5–10 min per sample. Shan et al. [60] used 30 s per image (image area:  $30 \times 20$  mm). Karlsson et al. [55] reports three different acquisition times for the respective instruments: < 1 min (image area:  $120 \times 120$  mm) with a Videometer instrument, 1 min (image height: 96 mm, image length: unspecified) with a Umbio Inspector and 5–10 min (image area:  $49 \times 55$  mm) using a Malvern instrument. Serranti et al. [58] analyzed 738 particles in 17 images using SISU ChemaXL, but analysis time was not reported. Based on manufacturer's specifications, we can assume that the scanning rate was 40 mm/s (image height: 2.8 mm).

A drastic reduction in analysis time is a clear strength of HSI. Particle recognition software reduces bias when analyzing particles with Raman and FT-IR, but it does not necessarily reduce analysis time as each particle must still be analyzed individually. Conversely, analysis time of imaging methods such as FPA-FTIR will be directly dependent on the area, not the particle number. While this is also true for HSI, analysis time is reported in seconds or minutes as compared to hours for FPA-FT-IR instruments. To illustrate this difference, we can directly compare scan times. An HSI system can cover  $240 \text{ mm}^2/\text{second}$  at a spatial resolution of  $60 \mu\text{m}$  (Videometer instrument, [55]).  $240 \text{ mm}^2$  is approximately equivalent to the surface area of one 47 mm diameter filter. Therefore, analyzing one filter takes only one second with HSI. To complete the same task, an FPA-FT-IR instrument with a scanning speed of  $4.9 \text{ mm}^2/\text{hour}$  ( $5.5 \mu\text{m}$  spatial resolution) would take 49 h. Spatial resolution is sacrificed for speed by using HSI. However, modifications such as adding a phototube can improve the spatial resolution [65] and thus render HSI competitive to other imaging techniques. HSI could also be advantageous for researches with limited resources both for the purchase of instrumentation and time spent on analysis.

### Data processing and quality control

Hyperspectral imagers produce large amounts of noisy three-dimensional data. Data processing can be divided into three processes: spectral pre-processing, pixel classification and image characterization for particle identification. Spectral pre-processing is needed to reduce noise and remove unimportant variation. Pixel classification, usually by chemometric models, compresses and interprets the data and is a central challenge for HSI [55, 56, 64]. The goal is to match the unknown spectra in the hyperspectral datacube to known spectra from a reference material. By identifying pixels containing synthetic polymer spectra, we can conclude which polymer type is present and localize polymers in the image. Particle size, morphology and number can then be assessed through image characterization. This can be done visually based on the model output (manual counting and categorization) or could be substituted by automated image analysis for particle counting.

Spectral preprocessing aims to reduce instrumental artefacts or differences which arise due to factors other than the chemical composition of the sample. An example of this is the amplitude of a spectrum: The absolute spectral reflectance values could be very high for white MPs, but low for dark blue MPs. The features of the spectrum which allow for chemical identification are the relationships between peaks, not the absolute spectral reflectance values. Removing variations in amplitude will allow models to focus on spectral characteristics which are inherent to polymer type, and not necessarily connected to other features like color. Preprocessing is considered an important step but there is marked variation in the use of preprocessing both generally [72] and among the studies in this review.

Preprocessing techniques used for HSI analysis of MP include standard normal variate (SNV) [58, 59], 1st or 2nd derivative [55, 57–59], multiple scatter correction (MSC) [55], mean centering (MC) [58, 59], smoothing, and baseline correction [54, 56]. Preprocessing can be broadly divided into two categories: set-independent (i.e., one-way) and set-dependent (i.e., two-way). Set-independent methods process each spectrum independently, that is to say based only on the features of each individual spectrum [72]. Methods which fall into this category are SNV, MC, derivatives, smoothing and baseline correction. Set-dependent methods such as MSC use features averaged over the set of spectra being analyzed. This yields different results based on the group of included spectra.

Preprocessing is important for both training and testing data. For analysis of unknown spectra, use of set-dependent methods will give different results based on each group of unknowns. For example, MSC will “mix” the signals from polymer and non-polymer regions and potentially remove important information. For this



reason, set-independent preprocessing methods such as smoothing and SNV are recommended [72]. MC is a set-independent method, but not always necessary for hyperspectral data. The goal of MC is to ensure that all variables are within comparable ranges. As noted by Lee et al. [72], this is typically not necessary for spectral datasets as all variables are wavelengths and thus fundamentally comparable. We can conclude that SNV, 1st or 2nd derivatives or smoothing (or combinations thereof) are suitable preprocessing methods for MP hyperspectral data. Exactly which combination of methods is appropriate will depend on the quality of the data. The reader is referred to Lee et al. [72] for a more detailed discussion of preprocessing methods.

Interestingly, Shan et al. [60] and Shan et al. [64] used a PCA as a preprocessing method to reduce dimensionality of the data. The first 5 principal components were extracted and used for classification. This would technically be a set-dependent preprocessing method but does not “average out” details between groups as an MSC would. However, PCA does not replace other preprocessing methods whose aim is to reduce noise and extraneous variation. SNV, 1st or 2nd derivative and/or smoothing could also be applied before the PCA. If dimensionality reduction is a high priority for the given application, PCA can serve as an additional preprocessing tool.

After pre-processing, spectra must be classified into distinct categories. For MP research, these categories are most often polymer type (e.g., polypropylene vs. polyethylene). The goal with any classification approach is to correctly classify pixels based on the spectra. This is typically done by analyzing known spectra (i.e., a test-set) and comparing the results of the classification with the identity of the samples. The ability of various techniques or models to classify unknown spectra can be reported using parameters such as precision (P), recall (R), sensitivity and specificity. Precision indicates how many of the positives (i.e., polymer spectra) are true positives, while recall, also called sensitivity, is the fraction of true positives which are correctly classified. Specificity is the fraction of all negatives which are true negatives. These parameters are reported as percentages and indicate how many mistakes are made, classifying non-plastic pixels as plastic or missing true plastic pixels. Reporting of P and R values is a good way to compare quality across techniques since both are independent of the analysis method and chemometric model. The same values can be reported for studies using other methods even if they do not produce similar spectral and spatial data to HSI. However, it bears mentioning that the sample size of the test set is an important metric. If the test set is large and diverse and the P and R values remain high (e.g., 95%), this is an indication of a robust model. Testing with

smaller test sets could lead to erroneously high P and R values. Sample sizes should be considered when making inter-study or inter-method comparisons.

Analysis methods to classify spectra included a custom-built spectral library matching algorithm, spectral angle mapper (SAM), partial least squares discriminant analysis (PLS-DA), Mahalanobis distance (MD), maximum likelihood (ML), and support vector machine (SVM).

Spectral library matching used by Atwood et al. [54] is based on the protocol developed by Schmidt et al. [56] who created a spectral matching algorithm called PlaMAPP (Plastic Mapper). The algorithm is akin to spectral library matching used by FT-IR and Raman instruments and compares sample spectra to reference spectra based on local minima after smoothing and baseline correction. A matching penalty is calculated as the distance between matched pairs of minima and further divided by the squared percentage of matched absorption bands. The reference library contained 105 spectra of 13 polymer types which constitute common plastics expected in environmental samples. A matching penalty for each pixel is calculated based on the comparison to reference spectra, and each pixel is classified as a specific polymer type based on threshold values.

The PlaMAPP algorithm worked reasonably well for identifying MP. Of all the particles identified, 75% were confirmed as true positives ( $P = 75.00$ ) while 25% were false positives. Misclassification of organic matter (e.g., biofouling, sedimentation, attachment) as plastic particles and noisy spectra approximating polymer spectra were identified as the two main reasons for the high rate of false positives. Underestimation of the number of MP was also a problem as PlaMAPP could not discern adjacent particles of the same polymer type. In addition, Schmidt et al. [56] discuss how large particles can reflect light from their sides creating an “aura” resulting in an overestimation of the size of the particle.

To avoid noise being classified as a polymer, Schmidt et al. [56] imposed a two-pixel threshold that requires two adjacent pixels to be of the same polymer to qualify as MP. This minimized false positives but also reduced the spatial resolution. The authors also corrected for other false positives by visually inspecting particles under a microscope which is not very robust as discussed above. Visual confirmation also adds manual steps making the process both subjective and longer. Also, they did not find a solution for the misclassification of adjacent particles as one particle.

Spectral Angle Mapper (SAM) is another spectral matching technique. It uses a reference vector and compares each pixel vector to the reference. The angle between these vectors is calculated and used to assign classes. The SAM classification model was used by Gallagher et al. [63] and Zhu et al. [65]. P and R values were



not reported. In the case of Gallagher et al. [63], only one polymer was investigated. The exact polymer used in the study could be imaged as a reference, making spectral matching a by SAM a simple and effective choice (see further discussion with PLS-DA).

Four studies used PLS-DA for classification of spectra: Karlsson et al. [55], Schonlau et al. [57], Serranti et al. [58] and Serranti and Fiore et al. [59]. PLS-DA is based on principal components analysis which extracts latent variables from a data matrix. In the case of PLS-DA, a regression is performed on the latent variables to predict the response variable (i.e., the polymer type). The goal is to find latent variables relevant for the prediction of the response variable, that is, spectral features which will correctly classify polymers. PLS-DA requires training data where the response variable is known. For MP analysis this means samples of known polymer type must be imaged to acquire representative spectra for different polymers. In all cases, HSI spectra of virgin polymers were used to train the models.

Performance was reported in different ways. Karlsson et al. [55] reported percent increase in particle detection as compared with visual counts. Percent increase was on average 65%, confirming that visual identification often underestimates the presence of MP. However, some negative percentages were also reported, showing that HSI was also potentially vulnerable to underestimation. Karlsson et al. [55] are critical of their own model, noting a marked decrease in performance when classifying weathered plastics as opposed to clean household items which have not been exposed to harsh environmental conditions. The authors hypothesize that using weathered plastics as reference materials could improve performance. It should also be noted that they identified up to 12 different polymer types. Including so many classes in a PLS-DA model makes classification very complex.

Serranti et al. [58] and Serranti and Fiore et al. [59] take a contrasting approach using only 3 and 4 polymer types respectively. Average sensitivity and specificity values were 99.9 and 100% respectively, however, the minimum particle sizes were 500  $\mu\text{m}$  [58] and 1000  $\mu\text{m}$  [59]. Large particles are easier to detect than small particles, as their larger surface area covers a greater number of pixels. In addition to using large MP, using fewer classes simplifies classification significantly. Under these conditions, it seems that PLS-DA outperforms spectral matching as described above.

Spectral matching uses fewer spectra which are representative for each class. As little as one spectrum can be used to define an entire class of, for example, polymers. Considering that MP are a highly diverse group of polymers, additives, and other chemicals, one single spectrum may not be representative of all possible MP spectra. PLS-DA models use large training sets which

can represent a wider variety of spectra. The class is then defined according to the variation in the training set. PLS-DA might therefore be inherently more robust against within-class variance. However, spectral matching encompasses a wide range of techniques and should not be discounted. Techniques can be used in combination and tailored to the specific challenges of the application. Shanmugam and Srinivasaperumal [73] provide a comprehensive review of spectral matching techniques which could prove useful for MP analysis.

In addition to PLS-DA, Support Vector Machine (SVM) is a common supervised classification method. SVM classifiers use hyperplanes to classify samples in high dimensional space. The hyperplane is described by an equation which maximizes the margins of the hyperplane to all classes. The nearest items constraining the hyperplane are the so-called support vectors which describe decision boundaries. SVM classifiers were applied in three studies [60, 61, 64], all of which employed ENVI (Exelis Visual Information Solutions, Boulder, Colorado), a software designed to handle and analyze hyperspectral data. Regions of interest are selected in an RGB rendering of the hyperspectral datacube. Spectra from these regions are then used as training data for classification of unknown spectra. *P* and *R* values for SVM models varied widely but mostly as a function of particle size. Generally, SVM performed better than the PlaMAPP model with *P* values between 90% and 100% for particles > 250  $\mu\text{m}$ . In a direct comparison Shan et al. [60] compared different models and found that SVM outperformed MD and ML.

The ENVI software is attractive as it specializes in handling hyperspectral data and provides tools for multivariate analysis. Other programs such as QGIS, SeaDAS developed by NASA, and SNAP (European Space Agency) offer similar solutions. These programs are intended for remote sensing applications but are equally useful for analyzing images from a benchtop instrument. They have the benefit of handling hyperspectral data in a user-friendly way. ENVI requires a paid license however the other programs mentioned are open source. Open-source tools are also available on Github, but some require more expertise to use. SIMCA (Sartorius AG) is another software tool which offers easy-to-use multivariate analysis, and has been recently applied to HSI analysis of MP [74]. SIMCA analysis is similar to a PLS-DA but creates independent models for each class. This reduces complexity and improves performance when there are multiple classes and high within-class variation [75]. SIMCA could therefore perform better if more polymer types are included as well as weathered plastics for training data.

Other approaches have been proposed but only applied theoretically. Convolutional neural networks have

shown promising results for classification of hyperspectral images. Chaczko et al. [76] manipulated an existing collection of hyperspectral images of textiles to mimic MP. A neutral network was applied to classify the fabricated MP spectra. Further exploration of classification methods could lead to improved detection of MP. Combining spectral and spatial data is another possibility [77]. Spatial data could help compensate for degraded spectra of weathered particles or weak spectral reflectance of small particles.

Two main challenges highlighted in multiple studies were the detection of small particles and the classification of dark particles. Particles  $> 300\ \mu\text{m}$  were reliably detected by Shan et al. [64]. For class sizes below  $300\ \mu\text{m}$ , P and R values were consistently lower (Fig. 6). Zhang et al. [61] reported an average precision and recall of 68.5% and 74.5%, respectively, for particles as small as  $100\ \mu\text{m}$ . This was dependent on the polymer type, with PS and PE having the best classification results. This is presumably because some polymers have more distinct spectral characteristics (optical fingerprints) than others, making them easier to identify. Zhu et al. [65] also reported that  $100\ \mu\text{m}$  particles could be reliably characterized. The decrease of model performance for smaller particles indicates that the spatial resolution of the camera begins to limit the classification ability of the model. When a particle is smaller than the area covered by one pixel, the resulting spectrum will be a combination of spectral reflectance from the particle and other materials in the pixel area.

Analyzing dark particles is another challenge [60, 65]. Precision decreased for black compared to white PE

particles, indicating that there were more false positives [60]. Zhu et al. [65] describes poor identification of grey, black and brown particles owing to a lower reflectance that results in ambiguous or noisy spectra. This implies that spectral data will be less sufficient for classification as spectral reflectance of particles decreases.

The approach to data analysis will be highly dependent on the experience of the analyst as well as the tools available to them (i.e. open source vs. licensed software). Models like PLS-DA and SVM can be executed in open source software and are relatively easy to learn for people with knowledge in other statistical analyses. All analyses are however dependent on a representative and comprehensive database of spectra from a variety of plastics: both weathered, biofouled and pristine, a variety of polymers, sizes shapes and colors (dark vs. light). A shared database of spectra could contribute to facilitating analysis, reducing the number of steps needed for any individual research group. More publications are emerging providing hyperspectral datasets for plastics [78, 79], but access could be improved by including HSI data on established sharing platforms such as OpenSpecy [80]. More information on performance comparing different strategies, as well as a well-developed protocol for implementation would also be beneficial for researchers in biology, chemistry, and ecotoxicology.

Existing methods could also benefit from the same evaluation of the methods discussed here. FPA-FT-IR uses similar classification models and could thus easily report similar quality parameters when analyzing standard samples. While some chemometric analysis has been performed, data are often exploratory in nature and do not provide similar parameters on model quality [81, 82]. The introduction of more standardized practices from chemometrics could improve quality assurance and quality control of both HSI and other spectroscopic methods.

## Challenges and Recommendations

The HSI systems covered in this review were unable to detect MP smaller than  $100\ \mu\text{m}$ . This is not unexpected considering that most hyperspectral cameras are intended for larger objects. To make HSI competitive with other methods, the spatial resolution must be improved. Modifying existing instruments with optical elements (e.g. stereomicroscopes) may provide a simple way to increase spatial resolution. Development of HSI cameras for MP analysis would allow customization based on the needs of MP analysis.

Spectral resolution on the other hand can likely be decreased without sacrificing performance, for instance by targeting wavelengths that are specific for synthetic polymers. Reducing spectral information will reduce computational demands and make analysis simpler. Various

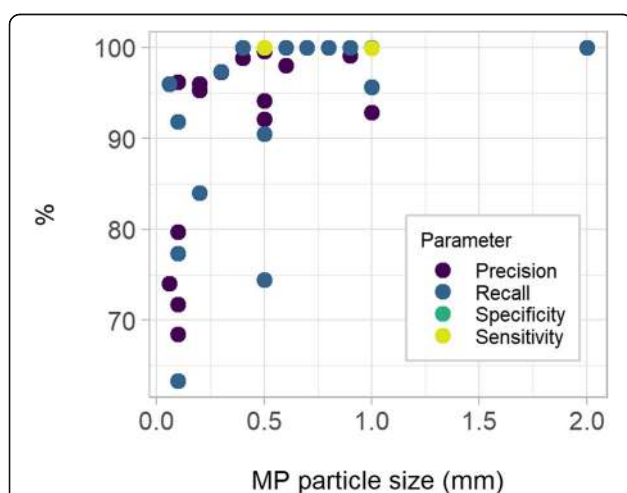


**Fig. 6** Precision, recall, sensitivity, and specificity of chemometric models used to identify MP. The x axis indicates the smallest particle size analyzed for each model. Precision, recall, sensitivity, and specificity are reported as percentages where 100% would indicate that the model made no classification errors for that parameter

examples from the remote sensing community show that plastic identification is possible using a multi spectral approach [37, 71]. Exactly how coarse the spectral resolution can be while still differentiating polymers is a question for future research.

Another concept we can adopt from remote sensing is the use of weathered plastics for creating reference spectra. Plastics sampled from the marine environment will have undergone varying degrees of weathering causing decreases in spectral amplitude and degradation of spectral features [83]. Furthermore, plastics found in nature come from a wide variety of sources and contain a diversity of additive chemicals. Biermann et al. [37] identified plastics floating on the ocean surface in satellite images from the Sentinel-2 multispectral instrument. A “floating debris index” was created using the known plastics as references. This reflectance index was used for identifying floating plastics in new images. Future research should compare the use of virgin and weathered plastics to see if more realistic training data can increase model performance.

Another opportunity for improvement would be the inclusion of spatial information such as the morphological features of MP to identify particles. None of the current models incorporate any spatial data for particle classification. While estimates of particle number, shape and size can be made from supervised analysis of hyperspectral images, this information is calculated after classification in a pixel-wise fashion based solely on spectral data. Particle recognition algorithms which use RGB images are already in use in FT-IR and Raman spectroscopy. Combining particle recognition with spectral data could result in a model which is more robust against degraded spectral features, either due to low spectral reflectance or heavy weathering of particles. As discussed, convolutional neural networks may be a candidate for combining spectral and spatial data.

Most studies included in this review reported quality control parameters which are largely absent in the current literature on MP identification and characterization. The use of models like SVM and PLS-DA requires a test dataset to evaluate the model's performance. Reporting performance parameters such as precision and recall through standardized testing provides important insight into how accurately MP are identified and characterized. It also serves as a basis for comparison between methods. FPA-FT-IR produces similar data to HSI (i.e., infrared spectra mapped over an area) and thus requires similar data handling techniques. The reporting of precision and recall for FPA-FT-IR and other MP methods could be done using spiked samples with known MP content, or by processing spectra from known MP. Including this information would allow even dissimilar analysis techniques to be compared.

**Table 4** Overview of common conclusions in the literature review

Conclusions	Source
Water reduces spectral reflectance, drying of particles is important	[61, 64]
SVM model outperforms PLS-DA, ML	[60, 64]
Dark particles are harder to detect	[60, 65]
ID of smaller particles is hindered by spatial resolution	[56, 60, 61, 64]
Weathered polymers have degraded spectra as compared with pristine polymers	[55, 62]
Reference polymers should be more diverse, include weathering and polymer mixtures	[65]
Over 90% of particles > 1 mm positively identified	[58, 60]
Addition of extra “class” for background or non-polymer material helped classification	[56, 59, 60]
Glass fiber filter is a suitable background material	[54–57, 64, 65]

Despite methodological differences, there were some common conclusions which appeared in multiple sources (Table 4). These general trends help to indicate best practices which can be adopted by other research groups intending to apply HSI to MP analysis. Some of the common threads relate to challenges while others provide key insights or solutions to the methodology.

## Conclusion

The studies assessed in this review indicate that HSI can positively identify MP consisting of various polymer types and size. Some exploration of color differences, background materials and spectral classification has provided a good framework for application of HSI to MP. Adjusting training data and spectral/spatial resolution could improve accuracy of classification models. Using more consistent terminology for reporting performance would facilitate comparisons between studies and methods and contribute to a better understanding of strengths and weaknesses of HSI. The main advantage of HSI over other methods is reduction in analysis time and objective analysis, (i.e., towards a more automated approach). Data analysis tools are still under development and not readily available to all researchers. With the development models made available on open source platforms, HSI could become a promising technique for further MP analysis.

## Abbreviations

ATR: Attenuated total reflectance; FOV: Field of view; FPA: Focal plane array; FT-IR: Fourier transform infrared spectroscopy; HSI: hyperspectral imaging; IR: Infrared; LOD: Limit of detection; MC: Mean centering; MD: Mahalanobis distance; ML: Maximum likelihood; MP: Microplastic; MSC: Multiple scatter correction; NIST: National Institute of Standards and Technology; PE: Polyethylene; PET: Polyethylene terephthalate; PLS-DA: Partial least squares discriminant analysis; PP: Polypropylene; PRISMA: Preferred Reporting

Items for Systematic Reviews and Meta-Analyses; PS: Polystyrene; PVC: Polyvinylchloride; Py-GC-MS: Pyrolysis gas chromatography mass spectrometry; QA/QC: Quality assurance/quality control; SAM: Spectral angle mapper; SNV: Standard normal variate; SVM: Support vector machine

### Acknowledgments

The authors would like to acknowledge Vishwesh Venkatraman (NTNU) for fruitful discussions on the subject of chemometric analysis and interpretation.

### Authors' contributions

AF conducted the literature search and reviewed all relevant articles. MW conducted an independent screening of literature results and collaborated with AF in choosing articles to be included in the review. AF read and extracted data from the included articles and synthesized the information therein. AF is the primary author of the text and creator of figures and Tables. MW and GJ have contributed to conceptualization and text structure as well as providing critical revision of the text and figures. All authors have read and approved the final manuscript.

### Funding

This study was funded by the Norwegian University of Science and Technology. Contributions from the Centre of Excellence at NTNU "AMOS" (NRC, Norwegian Research Council, Project 223254).

### Availability of data and materials

All data and materials used in the synthesis of this review can be found in the published article, with the exception of the protocol for performing the literature search which has been published on Zenodo [50] before conducting the search.

### Declarations

#### Competing interests

The authors declare that they have no competing interests.

Received: 17 March 2021 Accepted: 21 July 2021

Published online: 06 August 2021

### References

- Wagner M, Lambert S. Microplastics Are Contaminants of Emerging Concern in Freshwater Environments: An Overview. In: Wagner M, Lambert S, editors. *Freshwater microplastics: emerging environmental contaminants?* The Handbook of Environmental Chemistry: Springer Nature; 2018. p. 1–24. <https://doi.org/10.1007/978-3-319-61615-5>.
- Schell T, Rico A, Vighi M. Occurrence, Fate and Fluxes of Plastics and Microplastics in Terrestrial and Freshwater Ecosystems. In: de Voogt P, editor. *Reviews of Environmental Contamination and Toxicology*. Cham: 250: Springer; 2020. p. 1–43.
- Du J, Xu S, Zhou Q, Li H, Fu L, Tang J, et al. A review of microplastics in the aquatic environment: distribution, transport, ecotoxicology, and toxicological mechanisms. *Environ Sci Pollut Res*. 2020;27(11):11494–505. <https://doi.org/10.1007/s11356-020-08104-9>.
- Koelmans B, Pahl S, Backhaus T, Bessa F, van Calster G, Contzen N, et al. A scientific perspective on microplastics in nature and society: SAPEA; 2019.
- Ajith N, Arumugam S, Parthasarathy S, Manupoori S, Janakiraman S. Global distribution of microplastics and its impact on marine environment—a review. *Environ Sci Pollut Res*. 2020;27(21):25970–86. <https://doi.org/10.1007/s11356-020-09015-5>.
- GESAMP. Guidelines for the Monitoring and Assessment of Plastic Litter in the Ocean. *Journal Series GESAMP Reports and Studies*; 2019.
- Cole M, Lindeque P, Halsband C, Galloway TS. Microplastics as contaminants in the marine environment: a review. *Mar Pollut Bull*. 2011;62(12):2588–97. <https://doi.org/10.1016/j.marpolbul.2011.09.025>.
- Goetz AF, Vane G, Solomon JE, Rock BN. Imaging spectrometry for earth remote sensing. *Science*. 1985;228(4704):1147–53. <https://doi.org/10.1126/science.228.4704.1147>.
- Johnsen G, Volent Z, Dierssen H, Pettersen R, Van Ardelan M, Sørreide F, et al. Underwater hyperspectral imagery to create biogeochemical maps of seafloor properties. In: Watson J, Zielinski O, editors. *Subsea Optics and Imaging*. Electronic and Optical Materials: 46: Woodhead Publishing; 2013. p. 509–35.
- Lee K-J, Kang S, Kim MS, Noh S-H. Hyperspectral imaging for detecting defect on apples. In: 2005 ASAE Annual Meeting. 2005. Michigan: American Society of Agricultural and Biological Engineers; 2005. p. 053075.
- Lu G, Fei B. Medical hyperspectral imaging: a review. *J Biomed Opt*. 2014; 19(1):1–23. <https://doi.org/10.1117/1.JBO.19.9.096013>.
- Liu B, Liu Z, Men S, Li Y, Ding Z, He J, et al. Underwater Hyperspectral Imaging Technology and Its Applications for Detecting and Mapping the Seafloor: A Review. *Sensors*. 2020;20(17):e4962.
- Wu X, Li J, Yao L, Xu Z. Auto-sorting commonly recovered plastics from waste household appliances and electronics using near-infrared spectroscopy. *J Clean Prod*. 2020;246:e118732.
- Fu W, Min J, Jiang W, Li Y, Zhang W. Separation, characterization and identification of microplastics and nanoplastics in the environment. *Sci Total Environ*. 2020;721:e137561.
- Masura J, Baker J, Foster G, Arthur C. Laboratory Methods for the Analysis of Microplastics in the Marine Environment: Recommendations for quantifying synthetic particles in waters and sediments. National Oceanic and Atmospheric Administration; 2015. Report No.: NOAA Technical Memorandum NOS-OR&R-48.
- Hartmann NB, Hüffer T, Thompson RC, Hassellöv M, Verschoor A, Daugaard AE, et al. Are we speaking the same language? Recommendations for a definition and categorization framework for plastic debris. *Environ Sci Technol*. 2019;53(3):1039–47. <https://doi.org/10.1021/acs.est.8b05297>.
- Barrows AP, Christiansen KS, Bode ET, Hoellein TJ. A watershed-scale, citizen science approach to quantifying microplastic concentration in a mixed land-use river. *Water Res*. 2018;147:382–92. <https://doi.org/10.1016/j.watres.2018.10.013>.
- Hidalgo-Ruz V, Gutow L, Thompson RC, Thiel M. Microplastics in the marine environment: a review of the methods used for identification and quantification. *Environ Sci Technol*. 2012;46(6):3060–75. <https://doi.org/10.1021/es2031505>.
- Lenz R, Enders K, Stedmon CA, Mackenzie DM, Nielsen TG. A critical assessment of visual identification of marine microplastic using Raman spectroscopy for analysis improvement. *Mar Pollut Bull*. 2015;100(1):82–91. <https://doi.org/10.1016/j.marpolbul.2015.09.026>.
- Song YK, Hong SH, Jang M, Han GM, Rani M, Lee J, et al. A comparison of microscopic and spectroscopic identification methods for analysis of microplastics in environmental samples. *Mar Pollut Bull*. 2015;93(1–2):202–9. <https://doi.org/10.1016/j.marpolbul.2015.01.015>.
- Käppler A, Fischer D, Oberbeckmann S, Schernewski G, Labrenz M, Eichhorn K-J, et al. Analysis of environmental microplastics by vibrational microspectroscopy: FTIR, Raman or both? *Anal Bioanal Chem*. 2016;408(29): 8377–91. <https://doi.org/10.1007/s00216-016-9956-3>.
- Hermabessiere L, Himber C, Boricaud B, Kazour M, Amara R, Cassone A-L, et al. Optimization, performance, and application of a pyrolysis-GC/MS method for the identification of microplastics. *Anal Bioanal Chem*. 2018; 410(25):6663–76. <https://doi.org/10.1007/s00216-018-1279-0>.
- Fischer M, Scholz-Böttcher BM. Simultaneous trace identification and quantification of common types of microplastics in environmental samples by pyrolysis-gas chromatography–mass spectrometry. *Environ Sci Technol*. 2017;51(9):5052–60. <https://doi.org/10.1021/acs.est.6b06362>.
- Picó Y, Barceló D. Pyrolysis gas chromatography-mass spectrometry in environmental analysis: focus on organic matter and microplastics. *TrAC Trend Anal Chem*. 2020;130:e115964.
- Hayany BE, Fels LE, Quénéa K, Dignac M-F, Rumpel C, Gupta VK, et al. Microplastics from lagooning sludge to composts as revealed by fluorescent staining-image analysis, Raman spectroscopy and pyrolysis-GC/MS. *J Environ Manage*. 2020;275:e111249.
- Renner G, Schmidt TC, Schram J. Analytical methodologies for monitoring micro(nano)plastics: Which are fit for purpose? *Curr Opin Environ Sci Health*. 2018;1:55–61. <https://doi.org/10.1016/j.coesh.2017.11.001>.
- Oßmann BE, Sarau G, Holtmannspötter H, Pischetsrieder M, Christiansen SH, Dicke W. Small-sized microplastics and pigmented particles in bottled mineral water. *Water Res*. 2018;141:307–16. <https://doi.org/10.1016/j.watres.2018.05.027>.
- Primpke S, Christiansen SH, Cowger W, De Frond H, Deshpande A, Fischer M, et al. Critical Assessment of Analytical Methods for the Harmonized and Cost Efficient Analysis of Microplastics. *Appl Spectrosc*. 2020;74(9):1012–47. <https://doi.org/10.1177/0003702820921465>.



29. Frère L, Paul-Pont I, Moreau J, Soudant P, Lambert C, Huvet A, et al. A semi-automated Raman micro-spectroscopy method for morphological and chemical characterizations of microplastic litter. *Mar Pollut Bull.* 2016;113(1–2):461–8.
30. Xu J-L, Thomas KV, Luo Z, Gowen AA. FTIR and Raman imaging for microplastics analysis: State of the art, challenges and prospects. *TrAC Trends Anal Chem.* 2019;119:115629. <https://doi.org/10.1016/j.trac.2019.115629>.
31. Mintenig S, Int-Veen I, Löder MG, Primpke S, Gerdt G. Identification of microplastic in effluents of waste water treatment plants using focal plane array-based micro-Fourier-transform infrared imaging. *Water Res.* 2017;108:365–72. <https://doi.org/10.1016/j.watres.2016.11.015>.
32. Primpke S, Lorenz C, Rascher-Friesenhausen R, Gerdt G. An automated approach for microplastics analysis using focal plane array (FPA) FTIR microscopy and image analysis. *Anal Methods.* 2017;9(9):1499–511. <https://doi.org/10.1039/C6AY02476A>.
33. Löder MGJ, Kuczera M, Mintenig S, Lorenz C, Gerdt G. Focal plane array detector-based micro-Fourier-transform infrared imaging for the analysis of microplastics in environmental samples. *Environ Chem.* 2015;12(5):563–81. <https://doi.org/10.1071/EN14205>.
34. Goetz AFH. Three decades of hyperspectral remote sensing of the Earth: A personal view. *Remote Sens Environ.* 2009;113:55–S16. <https://doi.org/10.1016/j.rse.2007.12.014>.
35. Johnsen G, Ludvigsen M, Sørensen A, Aas LMS. The use of underwater hyperspectral imaging deployed on remotely operated vehicles-methods and applications. *IFAC-PapersOnLine.* 2016;49(23):476–81. <https://doi.org/10.1016/j.ifacol.2016.10.451>.
36. Buckingham R, Staenz K. Review of current and planned civilian space hyperspectral sensors for EO. *Can J Remote Sens.* 2008;34(sup1):S187–97.
37. Biermann L, Clewley D, Martinez-Vicente V, Topouzelis K. Finding Plastic Patches in Coastal Waters using Optical Satellite Data. *Sci Rep.* 2020;10:e5364.
38. Garaba SP, Aitken J, Slat B, Dierssen HM, Lebreton L, Zielinski O, et al. Sensing ocean plastics with an airborne hyperspectral shortwave infrared imager. *Environ Sci Technol.* 2018;52(20):11699–707. <https://doi.org/10.1021/acs.est.8b02855>.
39. Topouzelis K, Papageorgiou D, Karagaitanakis A, Papakonstantinou A, Arias BM. Remote Sensing of Sea Surface Artificial Floating Plastic Targets with Sentinel-2 and Unmanned Aerial Systems (Plastic Litter Project 2019). *Remote Sens.* 2020;12(12):e2013.
40. Topouzelis K, Papakonstantinou A, Garaba SP. Detection of floating plastics from satellite and unmanned aerial systems (Plastic Litter Project 2018). *Int J Appl Earth Obs Geoinf.* 2019;79:175–83. <https://doi.org/10.1016/j.jag.2019.03.011>.
41. Gonçalves G, Andriolo U, Pinto L, Bessa F. Mapping marine litter using UAS on a beach-dune system: a multidisciplinary approach. *Sci Total Environ.* 2020;706:e135742.
42. Smith A. A Pixel Is Not A Little Square, A Pixel Is Not A Little Square, A Pixel Is Not A Little Square. 1995. Report No.: Technical Memo 6.
43. Grahn H, Geladi P. Techniques and applications of hyperspectral image analysis: John Wiley & Sons; 2007. <https://doi.org/10.1002/9780470010884>.
44. Sun D-W. Hyperspectral imaging for food quality analysis and control: Elsevier; 2010.
45. Ramavaram HR, Kotichintala S, Naik S, Critchley-Marrows J, Isaiah OT, Pittala M, et al. Tracking ocean plastics using aerial and space borne platforms: Overview of techniques and challenges: Proceedings of the International Astronautical Congress, IAC; 2018.
46. Acuña-Ruz T, Uribe D, Taylor R, Amézquita L, Guzmán MC, Merrill J, et al. Anthropogenic marine debris over beaches: Spectral characterization for remote sensing applications. *Remote Sens Environ.* 2018;217:309–22. <https://doi.org/10.1016/j.rse.2018.08.008>.
47. Gupta N. Development of staring hyperspectral imagers. In: 2011 IEEE Applied Imagery Pattern Recognition Workshop (AIPR); 11–13 Oct 2011. Washington, DC: Institute of Electrical and Electronics Engineers; 2011. p. 1–8.
48. Smith BC. Fundamentals of Fourier transform infrared spectroscopy. 2nd ed. Boca Raton: CRC Press; 2011. <https://doi.org/10.1201/b10777>.
49. Workman J, Weyer L. Practical guide and spectral atlas for interpretive near-infrared spectroscopy: CRC press; 2012. <https://doi.org/10.1201/b11894>.
50. Faltynkova A, Wagner M, Johnsen G. Hyperspectral Imaging: An early systematic review of emerging applications for rapid microplastic analysis. Zenodod [Internet]. 2020. Available from: <https://doi.org/10.5281/zenodo.3862062>.
51. Moher D, Liberati A, Tetzlaff J, Altman DG, Group P. Preferred reporting items for systematic reviews and meta-analyses: the PRISMA statement. *PLoS Med.* 2009;6(7):e1000097. <https://doi.org/10.1371/journal.pmed.1000097>.
52. Ouzzani M, Hammady H, Fedorowicz Z, Elmagarmid A. Rayyan—a web and mobile app for systematic reviews. *Syst Rev.* 2016;5(1):1–10.
53. Provencher JF, Covernton GA, Moore RC, Horn DA, Conkle JL, Lusher AL. Proceed with caution: The need to raise the publication bar for microplastics research. *Sci Total Environ.* 2020;748:141426. <https://doi.org/10.1016/j.scitotenv.2020.141426>.
54. Atwood EC, Falcieri FM, Piehl S, Bochow M, Matthies M, Franke J, et al. Coastal accumulation of microplastic particles emitted from the Po River, Northern Italy: Comparing remote sensing and hydrodynamic modelling with in situ sample collections. *Mar Pollut Bull.* 2019;138:561–74. <https://doi.org/10.1016/j.marpolbul.2018.11.045>.
55. Karlsson TM, Grahn H, van Bavel B, Geladi P. Hyperspectral imaging and data analysis for detecting and determining plastic contamination in seawater filtrates. *JNIRS.* 2016;24(2):141–9.
56. Schmidt LK, Bochow M, Imhof HK, Oswald SE. Multi-temporal surveys for microplastic particles enabled by a novel and fast application of SWIR imaging spectroscopy - Study of an urban watercourse traversing the city of Berlin, Germany. *Environ Pollut.* 2018;239:579–89. <https://doi.org/10.1016/j.envpol.2018.03.097>.
57. Schonlau C, Karlsson TM, Rot e A, Nilsson H, Engwall M, et al. Microplastics in sea-surface waters surrounding Sweden sampled by manta trawl and in-situ pump. *Mar Pollut Bull.* 2020;153:111019.
58. Serranti S, Palmieri R, Bonifazi G, Cozar A. Characterization of microplastic litter from oceans by an innovative approach based on hyperspectral imaging. *Waste Manag.* 2018;76:117–25. <https://doi.org/10.1016/j.wasman.2018.03.003>.
59. Serranti S, Fiore L, Bonifazi G, Takeshima A, Takeuchi H, Kashiwada S. Microplastics characterization by hyperspectral imaging in the SWIR range. In: Kimata M, Valenta CR, editors. Proceedings Volume 11197, SPIE Future Sensing Technologies; 12 Nov 2019; Tokyo, Japan. Bellingham: SPIE; 2019. p. e1119710.
60. Shan J, Zhao J, Liu L, Zhang Y, Wang X, Wu F. A novel way to rapidly monitor microplastics in soil by hyperspectral imaging technology and chemometrics. *Environ Pollut.* 2018;238:121–9. <https://doi.org/10.1016/j.envpol.2018.03.026>.
61. Zhang Y, Wang X, Shan J, Zhao J, Zhang W, Liu L, et al. Hyperspectral Imaging Based Method for Rapid Detection of Microplastics in the Intestinal Tracts of Fish. *Environ Sci Technol.* 2019;53(9):5151–8. <https://doi.org/10.1021/acs.est.8b07321>.
62. Balsi M, Esposito S, Moroni M. Hyperspectral characterization of marine plastic litters. In: IEEE International Workshop on Metrology for the Sea; Learning to Measure Sea Health Parameters (MetroSea) [Internet]; 8–10 Oct. 2018. Bari: Institute of Electrical and Electronics Engineers; 2019. p. 28–32.
63. Gallagher MJ, Buchman JT, Qiu TA, Zhi B, Lyons TP, y KM, et al. Release, detection and toxicity of fragments generated during artificial accelerated weathering of CdSe/ZnS and CdSe quantum dot polymer composites. *Environ Sci Nano.* 2018;5(7):1694–710. <https://doi.org/10.1039/C8EN00249E>.
64. Shan J, Zhao J, Zhang Y, Liu L, Wu F, Wang X. Simple and rapid detection of microplastics in seawater using hyperspectral imaging technology. *Anal Chim Acta.* 2019;1050:161–8. <https://doi.org/10.1016/j.jaca.2018.11.008>.
65. Zhu C, Kanaya Y, Nakajima R, Tsuchiya M, Nomaki H, Kitahashi T, et al. Characterization of microplastics on filter substrates based on hyperspectral imaging: Laboratory assessments. *Environ Pollut.* 2020;263:e114296.
66. CytoViva Inc. CytoViva Hyperspectral Microscope [Internet]. CytoViva Inc; [date unknown] [cited 2021 Jul 15]. Available from: <https://cytoviva.com/products/hyperspectral-imaging-2/hyperspectral-imaging/>.
67. Nigmatzyanova L, Fakhruillina R. Dark-field hyperspectral microscopy for label-free microplastics and nanoplastics detection and identification in vivo: A *Caenorhabditis elegans* study. *Environ Pollut.* 2021;271:e116337.
68. Mattsson K, Johnson EV, Malmendal A, Linse S, Hansson LA, Cedervall T. Brain damage and behavioural disorders in fish induced by plastic nanoparticles delivered through the food chain. *Sci Rep.* 2017;7(1):e11452.
69. Fakhruillina R, Nigmatzyanova L, Fakhruillina G. Dark-field/hyperspectral microscopy for detecting nanoscale particles in environmental nanotoxicology research. *Sci Total Environ.* 2021;772:145478. <https://doi.org/10.1016/j.scitotenv.2021.145478>.
70. Volent Z, Johnsen G, Sigernes F. Microscopic hyperspectral imaging used as a bio-optical taxonomic tool for micro-and macroalgae. *Appl Opt.* 2009;48(21):4170–6. <https://doi.org/10.1364/AO.48.004170>.



71. Hibbitts CA, Bekker D, Hanson T, Knuth D, Goldberg A, Ryan K, et al. Dual-band discrimination and imaging of plastic objects. In: Bishop S, Isaacs J, editors. Proceedings Volume 11012, Detection and Sensing of Mines, Explosive Objects, and Obscured Targets XXIV, SPIE Defense + Commercial Sensing; 14–18 April 2019. Baltimore: SPIE; 2019. p. e1101211.
72. Lee LC, Liong C-Y, Jemain AA. Partial least squares-discriminant analysis (PLS-DA) for classification of high-dimensional (HD) data: a review of contemporary practice strategies and knowledge gaps. *Analyst*. 2018; 143(15):3526–39. <https://doi.org/10.1039/C8AN00599K>.
73. Shanmugam S, Srinivasaperumal P. Spectral matching approaches in hyperspectral image processing. *Int J Remote Sens*. 2014;35(24):8217–51. <https://doi.org/10.1080/01431161.2014.980922>.
74. Vidal C, Pasquini C. A comprehensive and fast microplastics identification based on near-infrared hyperspectral imaging (HSI-NIR) and chemometrics. *Environ Pollut*. 2021;285:e117251.
75. Bylesjö M, Rantalainen M, Cloarec O, Nicholson JK, Holmes E, Trygg J. OPLS discriminant analysis: combining the strengths of PLS-DA and SIMCA classification. *J Chemom*. 2006;20(8–10):341–51. <https://doi.org/10.1002/cem.1006>.
76. Chaczko Z, Wajs-Chaczko P, Tien D, Haidar Y. Detection of Microplastics Using Machine Learning. In: 18th International Conference on Machine Learning and Cybernetics [Internet]. Kobe: IEEE Computer Society Proceedings of 2019 International Conference on Machine Learning and Cybernetics; [1–8]; 2019.
77. Zhang H, Li Y, Zhang Y, Shen Q. Spectral-spatial classification of hyperspectral imagery using a dual-channel convolutional neural network. *Remote Sens Lett*. 2017;8(5):438–47. <https://doi.org/10.1080/2150704X.2017.1280200>.
78. Knaeps E, Sterckx S, Strackx G, Mijndonckx J, Moshtaghi M, Garaba SP, et al. Hyperspectral-reflectance dataset of dry, wet and submerged marine litter. *Earth System Science Data*. 2021;13(2):713–30. <https://doi.org/10.5194/essd-13-713-2021>.
79. Tasseron P, van Emmerik T, Peller J, Schreyers L, Biermann L. Advancing Floating Macroplastic Detection from Space Using Experimental Hyperspectral Imagery. *Remote Sens*. 2021;13(12):2335. <https://doi.org/10.3390/rs13122335>.
80. Cowger W, Steinmetz Z, Gray A, Munno K, Lynch J, Hapich H, et al. Microplastic Spectral Classification Needs an Open Source Community: Open Specy to the Rescue! *Anal Chem*. 2021;93(21):7543–8. <https://doi.org/10.1021/acs.analchem.1c00123>.
81. Wander L, Vianello A, Vollertsen J, Westad F, Braun U, Paul A. Exploratory analysis of hyperspectral FTIR data obtained from environmental microplastics samples. *Anal Methods*. 2020;12(6):781–91. <https://doi.org/10.1039/C9AY02483B>.
82. Zhang J, Tian K, Lei C, Min S. Identification and quantification of microplastics in table sea salts using micro-NIR imaging methods. *Anal Methods*. 2018;10(24):2881–7. <https://doi.org/10.1039/C8AY00125A>.
83. Garaba SP, Dierssen HM. Hyperspectral ultraviolet to shortwave infrared characteristics of marine-harvested, washed-ashore and virgin plastics. *Earth Sys Sci Data*. 2020;12(1):77–86. <https://doi.org/10.5194/essd-12-77-2020>.

## Publisher's Note

Springer Nature remains neutral with regard to jurisdictional claims in published maps and institutional affiliations.

**Submit your manuscript to a SpringerOpen<sup>®</sup> journal and benefit from:**

- Convenient online submission
- Rigorous peer review
- Open access: articles freely available online
- High visibility within the field
- Retaining the copyright to your article

---

Submit your next manuscript at ► [springeropen.com](https://www.springeropen.com)